Atmos. Meas. Tech. Discuss., 6, 10057–10079, 2013
www.atmos-meas-tech-discuss.net/6/10057/2013/
doi:10.5194/amtd-6-10057-2013
© Author(s) 2013. CC Attribution 3.0 License.

Atmospheric Measurement Techniques Discussions

This discussion paper is/has been under review for the journal Atmospheric Measurement Techniques (AMT). Please refer to the corresponding final paper in AMT if available.

Critical evaluation of cloud contamination in the MISR aerosol products using MODIS cloud masking products

Y. Shi[1], **J. Zhang**[1], **J. S. Reid**[2], **B. Liu**[3], **and E. J. Hyer**[2]

[1]Department of Atmospheric Science, University of North Dakota, Grand Forks, ND, USA
[2]Marine Meteorology Division, Naval Research Laboratory, Monterey, CA, USA
[3]Department of Computer Science, University of North Dakota, Grand Forks, ND, USA

Received: 1 October 2013 – Accepted: 18 October 2013 – Published: 20 November 2013

Correspondence to: Y. Shi (yingxi.shi@my.und.edu) and J. Zhang (jzhang@aero.und.edu)

Published by Copernicus Publications on behalf of the European Geosciences Union.

Abstract

For the first time, using the Terra Moderate Resolution Imaging Spectroradiometer (MODIS)-based cloud screening methods, we have evaluated the impacts of cloud contamination on the Terra Multi-angle Imaging Spectroradiometer (MISR) aerosol optical depth (AOD) product. Our study, based on one year of collocated MISR and MODIS data, suggests that cloud contamination exists in both over-water and over-land MISR AOD data with heavier cloud contamination occurring over the high latitude Southern hemispheric oceans. On average globally, our study shows that thin cirrus cloud contamination introduces a possible ~0.01 high bias for the over-water MISR AOD retrievals. Over the mid to high latitude oceans and Southeast Asia, this number increases to 0.015–0.02. However, biases much larger than this mean value are found in individual retrievals. This study suggests that cloud-clearing methods using observations from MISR alone, which has only visible and near infrared channels, may not be sufficient. Measurements from MODIS can be applied to assist cloud-clearing of the MISR aerosol retrievals. Cloud screening algorithms based on multi-sensor approaches are feasible and should be considered for current and future satellite aerosol studies.

1 Introduction

The Multi-angle Imaging Spectroradiometer (MISR) instrument has been successfully applied to observe and study atmospheric aerosols for over a decade (e.g., Kahn et al., 2005). Featuring nine unique camera angles, MISR observations have been used to retrieve aerosol optical properties over most surface types, including bright surfaces, which thwart many other passive sensors (Diner et al., 1998; Kahn et al., 2010). One of the known issues for satellite aerosol products, including the MISR aerosol products, is cloud contamination (e.g., Zhang et al., 2005; Kahn et al., 2010). Although extensive research efforts have been attempted to study the impacts of cloud artifacts and cloud

AMTD
6, 10057–10079, 2013

contamination to aerosol retrievals from other sensors such as Moderate Resolution Imaging Spectroradiometer (MODIS) (Zhang et al., 2005; Hyer et al., 2011; Shi et al., 2011b; Toth et al., 2013) and Advanced Very High Resolution Radiometer (AVHRR) (Zhao et al., 2013), the impacts of cloud contamination on MISR aerosol products have not been fully explored or quantified. We do know that over ocean AODs from standard operational MODIS and MISR products have positive biases as large as 0.04, or roughly one-third of mean background AOD values (Zhang and Reid, 2010). This is in stark contrast to the accuracy requirement commonly professed by climate scientists of 0.01 (CCSP, 2009).

As suggested from previous studies, effective cloud screening for aerosol retrieval requires sophisticated algorithms and multispectral visible and infrared radiance data (e.g., Remer et al., 2005). However, MISR lacks channels in the near and far infrared region where cirrus clouds are most easily detected. Cloud screen algorithms for MISR using MISR data have been based on cloud-induced perturbations in either spectral radiance or angular dependent radiance values with the assistance of a reflected layer height technique (e.g., Kahn et al., 2007). A recent study by Witek et al. (2013) has extended the effort by using a much finer resolution (1.1 km) clear flag included in the MISR aerosol products for cloud-clearing of MISR AOD retrievals, vastly lowering MISR AODs to be in line with the Navy MODIS data assimilation grade product. However, cloud detection may be incomplete with the use of only visible and near IR channels, especially for thin clouds over bright surfaces. On board the same satellite platform as MISR, MODIS has a total of 36 spectral channels, including cirrus cloud sensitive channels as well as infrared channels, which provide an enhanced capability of detecting the presence of clouds in an observed scene (e.g., Ackerman et al., 1998). However, we have yet to find any published results on evaluation of cloud contamination in the MISR retrieval AOD data that takes advantage of collocated Terra-MODIS cloud masking data. In this study, using the Level 2 cloud masking products from Terra MODIS, we evaluated the existence of cloud contamination in the Terra MISR aerosol

AMTD
6, 10057–10079, 2013

products and evaluate different methods for eliminating cloud contamination from MISR aerosol products.

2 Data and methodology

2.1 Aerosol Robotic Network (AERONET) sun photometer data

The Aerosol Robotic Network (AERONET) is a federated network of sun photometer instruments deployed in several hundred locations across the globe. The AERONET sun photometers measure solar irradiance at multiple wavelengths, and can be used for very accurate estimates of AOD, as well as additional aerosol optical properties. With a reported uncertainty of 0.015, the AERONET AOD data are commonly used as a benchmark for validating satellite aerosol retrievals (Holben et al., 1998). For this study, 7 yr (2001–2007) of Level 2 AERONET data were used.

2.2 MISR aerosol products

MISR measures radiance in 4 spectral bands in the visible and near infrared (446.4, 557.5, 671.7, and 866.4 nm), with 9 cameras pointed at different angles along the sub-satellite track. Version 22 MISR aerosol products include AOD, aerosol particle size and shape, as well as other ancillary data at a spatial resolution of 17.6 km × 17.6 km. Validated against AERONET data, uncertainties in the MISR AOD product are on the order of 0.05 or $0.2 \times \mathrm{AOD}_{\mathrm{AERONET}}$ (e.g., Kahn et al., 2005). Cloud contamination in the MISR AOD data has been mentioned (Kahn et al., 2010), but has not been fully investigated using means like the MODIS cloud masking data. The baseline quality assurance steps (referred as "self-QAed" hereafter) in this study are based on data included in the MISR aerosol product. The following filters are used for the "Self-QAed" datasets:

– The Retrieval Applicability Mask flag (= 0) is used to exclude cloudy pixels.

AMTD
6, 10057–10079, 2013

– The Regional Classification Indicator (= 0) is used for selecting retrievals above clear background region.

– The Aerosol Retrieval Success Flag (= 7) is used to ensure successful retrievals.

– The Regional Surface Type Indicator is used to separate over-land from over-water retrievals. We also used the Regional Surface Type Indicator to exclude potential problematic regions such as shallow/coastal waters and Polar Regions.

Note that within the MISR AOD product, a retrieval applicability mask is available at a 1.1 km resolution, for 9 camera angles and 4 spectral bands. Only the red and near IR bands are used for over water aerosol retrievals (Martonchik et al., 1998). This mask is in a much finer resolution than the 17.6 km AOD retrievals and includes environmental conditions such as "clear", "glitter-contaminated", "cloudy" and "topographically obscured". Using the clear indicator in the retrieval applicability mask, a clear flag fraction (CFF) can be calculated for each of the MISR AOD retrievals by taking the ratio of clear vs. total flags for a total of $16 \times 16 \times 9$ flags (9 angles, 16 by 16 at 1.1 km MISR pixels). Witek et al. (2013) discussed the possibility of using the MISR CFF (use CFF > 60 %) as a means of removing cloud contaminated MISR AOD retrievals. In this study, we also compared the MODIS-based MISR cloud screening method developed from this study, with the method included in Witek et al. (2013). The results are shown in Sect. 3.

The impacts of cloud contamination on the MISR aerosol product were evaluated using seven-years (2001–2007) of collocated AERONET, MODIS and MISR data sets. One year of collocated MODIS and MISR products (2007) were also used for evaluating various cloud masking methods spatially. MISR AOD values were collocated with AERONET data following the method presented in Zhang et al. (2006). Pairs of observations were recorded when the spatial distance between the MISR and AERONET data is within 0.3° (latitude/longitude), and the temporal difference is within ±30 min. The collocated MISR and AERONET data were further collocated with MODIS cloud mask data for the cloud clearing analysis for the MISR aerosol products (see Sect. 2.4).

AMTD
6, 10057–10079, 2013

2.3 Cloud screening methods using MISR data

The MISR cloud team has developed three independent cloud detection methods: Radiometric Camera-by-Camera Cloud Mask (RCCM), Stereoscopically Derived Cloud Mask (SDCM), and Angular Signature Cloud Mask (ASCM) (Diner et al., 1998). RCCM is based on a radiance threshold technique and produces cloud masks for each of the nine camera angles at a 1.1 km spatial resolution. The SDCM method is designed to retrieve the reflecting layer height, and is used, in combination with the RCCM method, to indicate the confidence level of clouds near or above a surface. The ASCM method utilizes the differences in angular-dependent Rayleigh scattering in the blue and red or near IR channels at forward-scattering directions between high clouds and the surface. It is designed for detecting high clouds and for clouds over ice and snow surfaces. Over land, ASCM is only applied over the ice and snow surfaces and its threshold is static at this moment. A sensitivity study showed that the ASCM method is not sensitive to cirrus clouds that have optical depths less than 0.5 (Di Girolamo and Davies, 1994).

Besides the three primary cloud detection methods mentioned above, two additional data-filtering procedures, angle-to-angle smoothness evaluation and angle-to-angle correlation evaluation, along with a brightness test, are also used to further remove possible contaminated observations for aerosol retrievals by the MISR aerosol team (Diner et al., 2001). Both methods are aimed to eliminate pixels with large radiance variations within each camera angle and among the nine camera angles.

2.4 Cloud screening methods using MODIS data

The MODIS instrument has a total of 36 spectral channels with spatial resolutions ranging from 250 to 1000 m. With additional channels centered at IR and the 1.375 µm channels, MODIS, in-comparison with MISR, has an enhanced capability of detecting the presence of clouds, especially thin cirrus clouds (Ackerman et al., 1998). The MODIS cloud mask products focus on representing a level of confidence of how unobstructed the satellite field of view is at the pixel level. A combination of 19 visible

AMTD
6, 10057–10079, 2013

and infrared spectral bands was used to perform a series of threshold and consistency tests to detect clouds. The MODIS MOD35 cloud mask indicates cloud status with one of four values, including "cloudy (CD)", "uncertain clear (UC)", "probably clear (PC)", and "confidently clear (CC)", at a 1 km resolution. The MODIS cloud mask product also includes other ancillary information such as detection of thin cirrus cloud, high cloud, surface shadow, cloud adjacency, sea ice, snow, and sun glint. In this study, collocated with the MISR aerosol products, the 1 km resolution cloud screening flags from the MODIS cloud mask products were used for cloud clearing of MISR scenes. The thin cirrus cloud flag, derived primarily from the 1.375 µm water vapor sensitive band (Gao and Kaufman, 2003), was also used in this study for detecting thin cirrus clouds.

The spatial resolution of the MODIS cloud masking data is 1 km. However, the geolocation data in the Terra MODIS cloud mask products have a spatial resolution of 5 km. Therefore, to speed up the processing time, the cloud mask data were first averaged to a 5 km × 5 km resolution providing occurrence ratio for each cloud status. The 5 km × 5 km Terra MODIS cloud-masking data were then collocated with the Terra MISR aerosol products, with the spatial and temporal differences between the two products set to 6 km and 30 min respectively. The spatial resolution for the Terra MISR aerosol retrievals is ~ 17.6 km, thus one MISR aerosol retrieval can be collocated with multiple MODIS cloud masking values. The occurrence ratios from the 5 km averages were further averaged to compute a total of four parameters for one MISR AOD retrieval: cloudy fraction (F_{cd}), uncertain clear fraction (F_{uc}), probably clear fraction (F_{pc}), and confidently clear fraction (F_{cc}). The collocated thin cirrus cloud flag was processed the same way to construct an additional parameter that represents the fraction of the thin cirrus cloud free regions at the MISR AOD resolution (F_{cirrus_free}).

Lastly, seven years (2001–2007) of collocated MISR and AERONET aerosol, as well as MODIS cloud masking products, were used to evaluate the impacts of various cloud screening methods to the MISR AOD retrievals. We also used one year of collocated Terra MISR aerosol and MODIS cloud masking products to investigate the impacts spatially.

AMTD
6, 10057–10079, 2013

3 Results: a case study

An example of potential cloud contamination in the MISR aerosol products is shown in Fig. 1, over remote southern oceans (~ 44° to 52° S and 124° to 136° W, on 3 January 2007), where a pristine marine environment is expected. Figure 1a shows the RGB image constructed using nadir-viewing MISR near IR, green and blue bands. Cloudy and clear regions are observed in the bottom and upper parts of Fig. 1a, respectively. Figure 1b is the corresponding MISR self-QAed AOD plot, with AOD values ranging from near zero to over one. The near homogeneous low AODs of less than 0.1 are found from cloud free oceans. Near cloud edges and within cloudy regions, AODs of 0.2–0.3 are more typically found. To better illustrate the relative location between cloud edges and the retrieved AODs, Fig. 1c was created by overlaying Fig. 1a (in aqua color) and Fig. 1b (in red color) in a false-color composite. Bright red colors indicate high AOD values. Most of the highest AOD retrievals (AODs greater than 0.3) are located within cloudy regions and higher AOD values of around 0.2 to 0.3 are found near the edge of clouds. Figure 1d shows the MODIS brightness temperature (BT). Retrievals that have AOD values above 0.8 are found within regions that have BT values lower than 255 K, a clear indication of cloud contamination. Figure 1e shows the MODIS cloud mask product at the 1 km resolution with each pixel flagged as one of the four cloudy conditions: CD, UC, PC, and CC. Regions with high AOD values are mostly associated with pixels that have PC, UC, or CD cloud flags. This concept is further demonstrated from Fig. 1f–i. Figure 1f shows the fraction of MODIS cloud mask data that are free from thin cirrus cloud contamination ($F_{\text{cirrus\_free}} = 100\,\%$), averaged in the MISR AOD resolution. Most thin cirrus cloud free regions ($F_{\text{cirrus\_free}} = 100\,\%$) are associated with low MISR AOD values of ~ 0.15 or less. Figure 1g is similar as Fig. 1f but was created using the PC flag. High AOD values of 0.2–0.3 are still observed when F_{pc} is set to above 0.8, suggesting that the PC flag may not be a good cloud-free-sky indicator. Using strict cut values of F_{cd} and F_{uc} ($F_{\text{cd}} < 10\,\%$ and $F_{\text{uc}} < 20\,\%$), Fig. 1h shows that most of the AODs larger than 0.3 were removed, although there are still some AODs

AMTD
6, 10057–10079, 2013

around 0.3 located between clouds in the bottom right of the image. Figure 1i shows the cloud clearing with the use of the F_{cc} filter ($F_{cc} > 20\,\%$), most high AOD retrievals are removed, showing that the F_{cc} filter can be effectively used for cloud screening of MISR data. Attempts were also made to filter out cloud contamination in the MISR AOD data using the MISR CFF data (Fig. 1j and k). The fraction of the clear flag within the scene is shown in Fig. 1j. Figure 1k shows the MISR AOD retrievals after applying the MISR CFF filter (CFF > 60 %) as used in Witek et al. (2013). Shown in Fig. 1k, high AOD retrievals at the bottom right of the image are removed, including a significant portion of cloud free AODs as identified by MODIS, causing a 75 % data loss. More importantly, some of the high AODs, located within the totally cloudy regions as seen from Fig. 1c, passed the MISR CFF filter. This case study suggests that the MISR CFF method can be used to remove cloud contaminated MISR AOD data, but may not be as effective as the MODIS-based method, and may be subjected to a significant data loss. Thus, we choose to use MODIS F_{cc} as the primary parameter for cloud-clearing of the MISR AOD retrievals. Shown from this case study, cloud contamination exists in MISR aerosol products, and MODIS cloud mask data can be used, effectively, to exclude most of the cloud contaminated MISR AOD data points, especially with the use of the MODIS F_{cc} filter.

3.1 Cloud screening using the MODIS cloud mask products

A statistical analysis was conducted to explore the relationships between the four fractional parameters derived from the MODIS cloud masking products (F_{cd}, F_{uc}, F_{pc}, and F_{cc}) and MISR AOD. Shown in Fig. 2 are the means and data distributions of MISR AOD values as functions of F_{cd}, F_{uc}, F_{pc}, and F_{cc} for both the over-water (Fig. 2a–d) and over-land (Fig. 2e–h) cases, with the fractional data density illustrated in color contours for every 10 % of a given fraction. Notice that fractional changes in F_{cd}, F_{uc}, F_{pc}, and F_{cc} indicate the probability of occurrence. For example, an increase of F_{cd} (F_{uc}) from 0 to 100 % indicates a change from an unknown cloudy or clear scene to a 100 % high (low) confident cloudy scene, while an increase of F_{cc} (F_{pc}) from 0 to 100 % means a change

AMTD
6, 10057–10079, 2013

from an unknown scene to a 100 % high (low) confident clear scene. In Fig. 2a, the mean MISR AODs show a decreasing trend as F_{cc} (e.g., percentage of clear regions) increases. In comparison, Fig. 2d shows an increasing trend in MISR AOD as F_{cd} (confident cloudy fraction) increases. Both Fig. 2a and d shows similar features as found in the MODIS Dark Target (DT) AOD data, a feature identified by Zhang et al. (2005) as cloud contamination in the MODIS DT aerosol products. Mixed information is shown in Fig. 2b (F_{pc}) and c (F_{uc}) when the detection of cloud and clear scenes is less certain, indicating that PC and UC flags are not good for use in cloud masking of MISR data. Figure 2e–h shows a similar analysis as Fig. 2a–d but for the over-land case. Again, decreasing/increasing trends are found for the F_{cc}/F_{cd} cases. Comparing the over-land mean MISR AOD at a confident clear sky (F_{cc} = 100 %, Fig. 2e) with the similar scenario for the over water case (Fig. 2a), a higher mean AOD value of 0.18 is found for the over-land case. In comparison, increasing F_{uc} and F_{cd} percentages to 100 % raises the over-land MISR AOD to values over 0.3 and 0.4, a clear indication of cloud contamination in the MISR AOD data. Suggested from Fig. 2, it is feasible to use F_{cc} for cloud filtering of the MISR aerosol products.

Using seven years of collocated MODIS, MISR and AERONET data (2001–2007), a sensitivity study was conducted to investigate different cloud filtering methods using F_{cd}, F_{uc}, F_{pc}, and F_{cc}. Tables 1 and 2 show the Root Mean Square Errors (RMSEs) and the Mean Absolute Error (MAE) of MISR AOD (validated against AERONET data), the fraction of data within the expected uncertainty range (0.05 or 0.2 × $AOD_{AERONET}$) (e.g., Kahn et al., 2010), as well as the data loss rates for nine cloud-filtering steps for over-ocean and -land cases respectively.

The RMSE is defined as:

$$\mathrm{RMSE} = \sqrt{\frac{1}{n}\sum_{n}\left(\mathrm{AOD}_{\mathrm{AERONET}} - \mathrm{AOD}_{\mathrm{MISR}}\right)^2}. \quad (1)$$

AMTD
6, 10057–10079, 2013

The MAE is defined as:

$$\mathrm{MAE} = \frac{1}{n}\sum_{n}\left(\left|\mathrm{AOD}_{\mathrm{AERONET}} - \mathrm{AOD}_{\mathrm{MISR}}\right|\right). \quad (2)$$

The nine scenarios are: self-QAed, $F_{cd} < 50\,\%$, $F_{cd} > 50\,\%$, $F_{uc} < 50\,\%$, $F_{uc} > 50\,\%$, $F_{cc} > 20\,\%$, $F_{cc} > 50\,\%$, $F_{cc} > 80\,\%$, and cirrus cloud free ($F_{\mathrm{cirrus\_free}} = 100\,\%$). Also, all F_{cc} cloud-filtering steps are combined with the cirrus cloud filter (thin cirrus cloud free) as well. There are two types of data loss counts presented. One is calculated based on the collocated MISR and AERONET data and the other is recorded using all available MISR AOD data in 2007. Using the $F_{cd} > 50\,\%$ filter, a more than 60 % increase in RMSE is found for MISR AOD retrievals over both land and ocean with 20 % less data that fall within the expected error range, while even for the $F_{uc} > 50\,\%$ filter, a 20 % increase in RMSE is shown globally, indicating that cloud contamination is physically identifiable in the MISR AOD data, causing a high bias to the AOD retrievals (also discussed later in the text).

For the over-ocean case, when increasing the F_{cc} filtering values from 20 to 80 %, a reduction in RMSE (compared to the self-QAed RMSE) from 15 to 27 % is found along with an increase in the fraction of data that falls within the expected error range. Over global land, increasing the F_{cc} filtering values from 20 to 80 % introduces an increase in RMSE reduction from 16 to 24 %, but with an increasing data loss rate from 15 to 27 % for all MISR AOD data. It is worth mentioning that after the thin cirrus cloud filter, a 0.006 reduction in RMSE is found over global oceans.

Figure 3 shows the spatial distributions of MISR AOD for year 2007 at a half-degree Lat/Lon resolution, using the self-QAed MISR data (Fig. 3a) and the MISR AOD after applying the 20 and 80 % F_{cc} cloud filters combined with the thin cirrus cloud filter ($F_{\mathrm{cirrus\_free}} = 100\,\%$) (Fig. 3b and c). Although the overall patterns are similar, differences are also visible (Fig. 3e and f). For example, the aerosol belt over the high latitude southern ocean from Fig. 3b and c is much reduced. Indeed, a similar AOD belt is also observed from the original MODIS aerosol data and can be reduced with stringent cloud screening and quality assurance steps (Shi et al., 2011a). Although other

AMTD
6, 10057–10079, 2013

factors could also contribute (Toth et al., 2013), we believe cloud contamination is one of the sources for causing the elevated AOD belt over southern oceans (Shi et al., 2011a). The decrease in mean MISR AOD is more pronounced with the F_{cc} cloud filter at $F_{cc} > 80\,\%$ compared with $F_{cc} > 20\,\%$. Similar suppression in AOD is also found in high latitude northern oceans, yet the reason is not known. Over the West Coast of North Africa, the AOD values are reduced in Fig. 3b and c comparing with Fig. 3a (also seen from Fig. 3e and f, which were created to represent the differences between the self-QAed and the cloud filtered MISR AODs). We suspect that thick aerosol plumes could be labeled as cloudy pixels and are excluded from the cloud-filtered datasets. To further investigate if the reduction in AOD values over the regions mentioned above is caused by the thin cirrus cloud screening, we have repeated the procedures and used only the self-QAed MISR data that passed the cirrus cloud filter ($F_{cirrus\_free} = 100\,\%$) for 2007 (Fig. 3d). Figure 3d shows that after the thin cirrus filter, the aerosol loadings over the focus area (West Coast of North Africa) remain at a similar magnitude as Fig. 3a. Thus, we believe the weakened AOD features over the west coast of North Africa could be caused by applying the confident clear cloud filtering. Also, a discontinuity is found between the over-ocean and over-land aerosol features along the West Coast of North Africa (e.g., Fig. 3c). We suspect that this discontinuity is caused by the differences in the over ocean vs. over land cloud screening algorithms from the MODIS cloud masking products.

3.2 A longer-term study of cloud contamination in the MISR AOD data using F_{cc} data

The monthly and zonal differences were evaluated between the MISR self-QAed AOD data and MISR AOD data sets with three different cloud-screening methods for 2007. Figure 4 shows the monthly and zonal mean deviations from the self-QAed MISR AOD data for three data sets: (1–2) MISR AOD after applying the $F_{cc} > 20\,\%$ and $80\,\%$ filters combined with the thin cirrus cloud filter and (3) MISR AOD after applying the thin cirrus cloud filter ($F_{cirrus\_free} = 100\,\%$).

AMTD
6, 10057–10079, 2013

Figure 4a shows the monthly mean of MISR AOD minus the self-QAed AOD over global oceans. When compared to the self-QAed MISR AOD data, the cirrus-free (F_{cirrus_free} = 100 %) data have mean MISR AOD values that are consistently 0.01 to 0.015 lower throughout the year. Although uncertainties exist in the MODIS 1.375 µm cirrus detection method (Gao et al., 2003; Pierce et al., 2010), it is possible that thin cirrus cloud contamination is present in the MISR AOD products that could introduce a high bias of ∼ 0.01 over global oceans. The thin cirrus related bias could reach 0.015–0.02 over oceans at mid to high latitudes. Although not shown in this paper, a higher bias of ∼ 0.02 was also found over Southeast Asia (15° S to 25° N, 90° E to 160° E). The F_{cc} cloud screening method combined with the thin cirrus cloud filter introduces a year round reduction in AOD of 0.02 to 0.06 depending on the thresholds, especially during May, June and July. Figure 4b is similar as Fig. 4a but for the over-land case. When compared with self-QAed MISR AOD values, the thin cirrus cloud filter introduces a ∼ 0.005 reduction in the averaged MISR AOD through February to August. The reduction is found to be around 0.005 to 0.015 when the F_{cc} filters are applied.

Figure 4c and d shows similar plots as Fig. 4a and b but for the differences in zonal mean AOD averaged every 5° latitude bin. Over global oceans, the F_{cc} filters introduce larger reductions in AOD occurring from 0° to 20° N and beyond 50° S with the largest reductions reach 0.05 and 0.07 for 20 % and 80 % F_{cc} cut off, respectively. After applying the F_{cc} filtering method, there is almost no MISR data available beyond 55° S. Over-land, while compared with the self-QAed MISR zonal mean AOD values, reductions in MISR AOD were also found globally after applying the F_{cc} screening method.

4 Recommendations and conclusion

In this study, using collocated MODIS cloud masking products, we have evaluated potential cloud contamination in the MISR aerosol products. We found that:

1. Cloud contamination exists in the MISR AOD data. Especially, thin cirrus cloud contamination introduces a possible mean AOD high bias of ∼ 0.01 over global

AMTD
6, 10057–10079, 2013

oceans and 0.015–0.02 over the mid to high latitudes and Southeast Asia. This study suggests that additional cloud screening methods are needed for using the MISR aerosol products for future studies.

2. New MISR cloud screening methods such as the MISR CFF method (Witek et al., 2013) have been developed to reduce cloud contamination in the MISR aerosol retrievals. However, with the use of only visible and near IR channels from MISR, such methods may still have difficulty in identifying thin cirrus clouds, even while excluding a substantial fraction of the observations. The MODIS cloud masking data can be effectively used for reducing cloud contamination in the MISR aerosol retrievals, and is more effective in removing thin cirrus cloud contaminated cloudy MISR aerosol retrievals in comparison with cloud screening methods using only MISR observations.

3. Cloud masking using MODIS data introduces some potential problems. For example, it is possible that some of the high AODs are misidentified as cloudy pixels and are removed by the MODIS-based cloud filtering methods when strict thresholds are used. A regional based cloud screening method may be needed for rescuing these misidentified heavy aerosol polluted scenes, through the combined used of MODIS and MISR data at the radiance level.

4. This project demonstrated that data from one sensor (MODIS) can be applied to another (MISR) for the development of an improved product. Thus, the farsighted developers of systems such as on Terra and within the A-train were correct in that the sensor combinations can result in improvements over any single sensor algorithm. This will pave the way for future algorithms, or even systems (such as NPP and EarthCARE), which require multiple sensors feeding single algorithms.

AMTD
6, 10057–10079, 2013

Acknowledgements. This research was funded by the Office of Naval Research Code 322 and the NASA Interdisciplinary Science Program. Yingxi Shi is funded by the NASA Earth and Space Science Fellowship Program. We also appreciate the MISR aerosol team and the NASA Langley Atmospheric Science Data Center for the MISR aerosol data. We thank the AERONET program for establishing and maintaining the AERONET sites used in this study.

References

Ackerman, S. A., Strabala, K. I., Menzel, W. P., Frey, R. A., Moeller, C. C., and Gumley, L. E.: Discriminating clear sky from clouds with MODIS, J. Geophys. Res.-Atmos., 103, 32141–32157, 1998.

CCSP: Atmospheric aerosol properties and climate impacts, a report by the US Climate Change Science Program and the Subcommittee on Global Change Research, edited by: Chin, M., Kahn, R. A., and Schwartz, S. E., National Aeronautics and Space Administration, Washington, D.C., USA, 128 pp., 2009.

Di Girolamo, L. and Davies, R.: A band-differenced angular signature technique for cirrus cloud detection, IEEE T. Geosci. Remote, 32, 890–896, 1994.

Diner, D. J., Beckert, J. C., Reilly, T. H., Bruegge, C. J., Conel, J. E., Kahn, R. A., Martonchik, J. V., Ackerman, T. P., Davies, R., Gerstl, S. A., Gordon, H. R., Muller, J., Myneni, R., Sellers, P. J., Pinty, B., and Verstraete, M. M.: Multi-angle Imaging SpectroRadiometer (MISR) instrument description and experiment overview, IEEE T. Geosci. Remote, 36, 1072–1087, 1998.

Diner, D. J., Abdou, W. A., Ackerman, T. P., Crean, K., Gordon, H. R., Kahn, R. A., Martonchik, J. V., McMuldroch, S., Paradise, S. R., Pinty, B., Verstraete, M. M., Wang, M., and West, R. A.: Level 2 aerosol retrieval algorithm theoretical basis, Jet Propulsion Laboratory, California Institute of Technology, 2001.

Gao, B. C. and Kaufman, Y. J.: Water vapor retrievals using Moderate Resolution Imaging Spectroradiometer (MODIS) near-infrared channels, J. Geophys. Res., 108, 4389, doi:10.1029/2002JD003023, 2003.

AMTD

6, 10057–10079, 2013

Holben, B. N., Eck, T. F., Slutsker, I., Tanré, D., Buis, J. P., Setzer, A., Vermote, E., Reagan, J. A., Kaufman, Y. J., Nakajima, T., Lavenu, F., Jankowiak, I., and Smirnov, A.: AERONET – a federated instrument network and data archive for aerosol characterization, Remote Sens. Environ., 66, 1–16, 1998.

Hyer, E. J., Reid, J. S., and Zhang, J.: An over-land aerosol optical depth data set for data assimilation by filtering, correction, and aggregation of MODIS Collection 5 optical depth retrievals, Atmos. Meas. Tech., 4, 379–408, doi:10.5194/amt-4-379-2011, 2011.

Kahn, R. A., Gaitley, A., B., Martonchik, J., Diner, D., Crean, K., and Holben, B. N.: MISR global aerosol optical depth validation based on two years of coincident AERONET observations, J. Geophys. Res., 110, D10S04, doi:10.1029/2004JD004706, 2005.

Kahn, R. A., Li, W.-H., Moroney, C., Diner, D. J., Martonchik, J. V., and Fishbein, E.: Aerosol source plume physical characteristics from space-based multiangle imaging, J. Geophys. Res., 112, D11205, doi:10.1029/2006JD007647, 2007.

Kahn, R. A., Gaitley, B. J., Garay, M. J., Diner, D. J., Eck, T. F., Smirnov, A., and Holbem, B. N.: Multiangle Imaging SpectroRadiometer global aerosol product assessment by comparison with Aerosol Robotic Network, J. Geophys. Res., 115, D23209, doi:10.1029/2010JD014601, 2010.

Martonchik, J. V., Diner, D. J., Kahn, R. A., Ackerman, T. P., Verstraete, M. M., Pinty, B., and Gordon, H. R.: Techniques for the retrieval of aerosol properties over land and ocean using multiangle imaging, IEEE T. Geosci. Remote, 36, 1212–1227, 1998.

Pierce, J. R., Kahn, R. A., Davis, M. R., and Comstock, J. M.: Detecting thin cirrus in Multiangle Imaging Spectroradiometer aerosol retrievals, J. Geophys. Res.-Atmos., V115, D8201, doi:10.1029/2009JD013019, 2001.

Remer, L. A., Kaufman, Y. J., Tanre, D., Mattoo, S., Chu, D. A., Martins, J. V., Li, R. R., Ichoku, C., Levy, R. C., Kleidman, R. G., Eck, T. F., Vermote, E., and Holben, B. N.: The MODIS aerosol algorithm, products and validation, J. Atmos. Sci., 62, 947–973, 2005.

Shi, Y., Zhang, J., Reid, J. S., Holben, B., Hyer, E. J., and Curtis, C.: An analysis of the collection 5 MODIS over-ocean aerosol optical depth product for its implication in aerosol assimilation, Atmos. Chem. Phys., 11, 557–565, doi:10.5194/acp-11-557-2011, 2011a.

Shi, Y., Zhang, J., Reid, J. S., Hyer, E. J., Eck, T. F., Holben, B. N., and Kahn, R. A.: A critical examination of spatial biases between MODIS and MISR aerosol products – application for potential AERONET deployment, Atmos. Meas. Tech., 4, 2823–2836, doi:10.5194/amt-4-2823-2011, 2011b.

AMTD
6, 10057–10079, 2013

Smirnov, A., Holben, B. N., Slutsker, I., Giles, D. M., McClain, C. R., Eck, T. F., Sakerin, S. M., Macke, A., Croot, P., Zibordi, G., Quinn, P. K., Sciare, J., Kinne, S., Harvey, M., Smyth, T. J., Piketh, S., Zielinski, T., Proshutinsky, A., Goes, J. I., Nelson, N. B., Larouche, P., Radionov, V. F., Goloub, P., Moorthy, K. K., Matarrese, R., Robertson, E. J., and Jourdin, F.: Maritime Aerosol Network as a component of Aerosol Robotic Network, J. Geophys. Res., 114, D06204, doi:10.1029/2008JD011257, 2009.

Toth, T. D., Zhang, J., Campbell, J. R., Reid, J. S., Shi, Y., Johnson, R. S., Smirnov, A., Vaughan, M. A., and Winker, D. M.: Investigating Enhanced Aqua MODIS Aerosol Optical Depth Retrievals over the Mid-to-High Latitude Southern Oceans through Intercomparison with Co-Located CALIOP, MAN, and AERONET Datasets, J. Geophys. Res.-Atmos., 118, 4700–4714, doi:10.1002/jgrd.50311, 2013.

Witek, M. L., Garay, M. J., Diner, D. J., and Smirnov, A.: Aerosol optical depths over oceans: a view from MISR retrievals and collocated MAN and AERONET in-situ observations, J. Geophys. Res.-Atmos., submitted, 2013.

Zhang, J. and Reid, J. S.: MODIS aerosol product analysis for data assimilation: assessment of level 2 aerosol optical thickness retrievals, J. Geophys. Res.-Atmos., 111, D22207, doi:10.1029/2005JD006898, 2006.

Zhang, J. and Reid, J. S.: A decadal regional and global trend analysis of the aerosol optical depth using a data-assimilation grade over-water MODIS and Level 2 MISR aerosol products, Atmos. Chem. Phys., 10, 10949–10963, doi:10.5194/acp-10-10949-2010, 2010.

Zhang, J., Reid, J. S., and Holben, B. N.: An analysis of potential cloud artifacts in MODIS over ocean aerosol optical thickness products, Geophys. Res. Lett., 32, L15803, doi:10.1029/2005GL023254, 2005.

Zhao, T. X. P., Chan, P. K., and Heidinger, A. K.: A global survey of the effect of cloud contamination on the aerosol optical thickness and its long-term trend derived from operational AVHRR satellite observations, J. Geophys. Res.-Atmos., in preparation, 2013.

AMTD
6, 10057–10079, 2013

Table 1. The RMSE, the fraction of data within the expected error (0.05 or 20 % of $AOD_{AERONET}$), and the data loss rates (both for the MISR AOD data that are collocated with AERONET data and for all MISR AOD data) under nine conditions over oceans. F_{cd} is the cloudy fraction, F_{uc} is the uncertainty clear fraction, and F_{cc} is the confident clear fraction. The thin cirrus cloud filter refers to thin cirrus cloud free (set F_{cirrus_free} = 100 %) as detected by MODIS.

	RMSE	MAE	% within the expected error	Data loss (collocated with AERONET)	Data loss (all MISR AOD data)
Self-QAed	0.082	0.059	59 %		
F_{cd} < 50 %	0.080	0.056	60 %		
F_{cd} > 50 %	0.137	0.107	40 %		
F_{uc} < 50 %,	0.084	0.059	60 %		
F_{uc} > 50 %,	0.096	0.081	43 %		
F_{cc} > 20 % + thin cirrus cloud filter	0.070	0.050	63 %	36 %	45 %
F_{cc} > 50 % + thin cirrus cloud filter	0.065	0.048	65 %	44 %	53 %
F_{cc} > 80 % + thin cirrus cloud filter	0.060	0.046	66 %	54 %	67 %
Thin cirrus cloud filter	0.076	0.054	62 %	22 %	21 %

AMTD
6, 10057–10079, 2013

Table 2. Similar to Table 1 but for the over land case.

	RMSE	MAE	% within the expected error	Data loss (collocated with AERONET)	Data loss (all MISR AOD data)
Self-QAed	0.143	0.072	61 %		
$F_{cd} < 50\,\%$	0.136	0.136	62 %		
$F_{cd} > 50\,\%$	0.262	0.144	42 %		
$F_{uc} < 50\,\%$,	0.136	0.069	62 %		
$F_{uc} > 50\,\%$,	0.400	0.189	47 %		
$F_{cc} > 20\,\%$ + thin cirrus cloud filter	0.120	0.066	63 %	25 %	15 %
$F_{cc} > 50\,\%$ + thin cirrus cloud filter	0.118	0.064	64 %	28 %	18 %
$F_{cc} > 80\,\%$ + thin cirrus cloud filter	0.109	0.060	65 %	38 %	27 %
Thin cirrus cloud filter	0.143	0.070	62 %	20 %	10 %

AMTD
6, 10057–10079, 2013

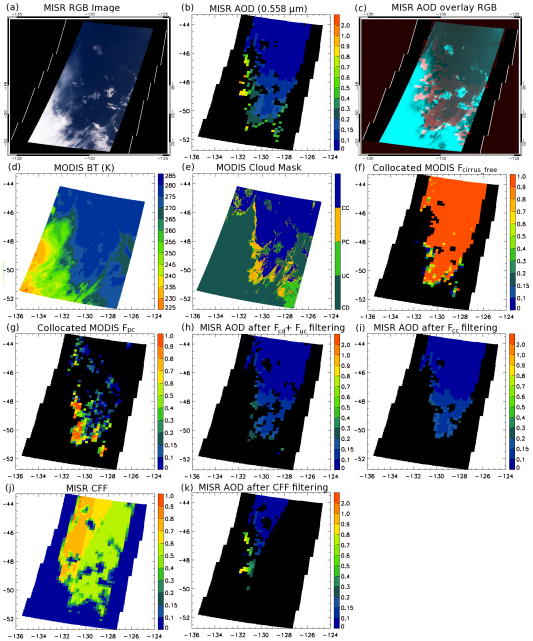

Fig. 1. A case study on 3 January 2007, over the remote oceans (44° to 52° S and 124° to 136° W), **(a)** RGB image created using the MISR Near IR, green and blue bands, **(b)** MISR AOD over the case study region, **(c)** Overlay of **(a)** on **(b)** where the intensity of red is correlated with the magnitude of the AOD, **(d)** MODIS brightness temperature (BT), **(e)** MODIS cloud mask, **(f)** collocated MODIS thin cirrus free cloud fraction (F_{cirrus_free}) in MISR AOD domain, **(g)** similar to **(f)** but for the collocated MODIS probably clear fraction (F_{pc}), **(h)** MISR AOD after passing the MODIS cloudy fraction (F_{cd}) < 10 % and the MODIS uncertainty clear fraction (F_{uc}) < 20 % cloud filters, **(i)** MISR AOD after passing the MODIS confident clear fraction (F_{cc}) > 20 % cloud filter, **(j)** MISR clear flag fraction (CFF), and **(k)** MISR AOD after passing the MISR CFF > 60 % filtering.

AMTD
6, 10057–10079, 2013

Critical evaluation of cloud contamination in the MISR aerosol products

Y. Shi et al.

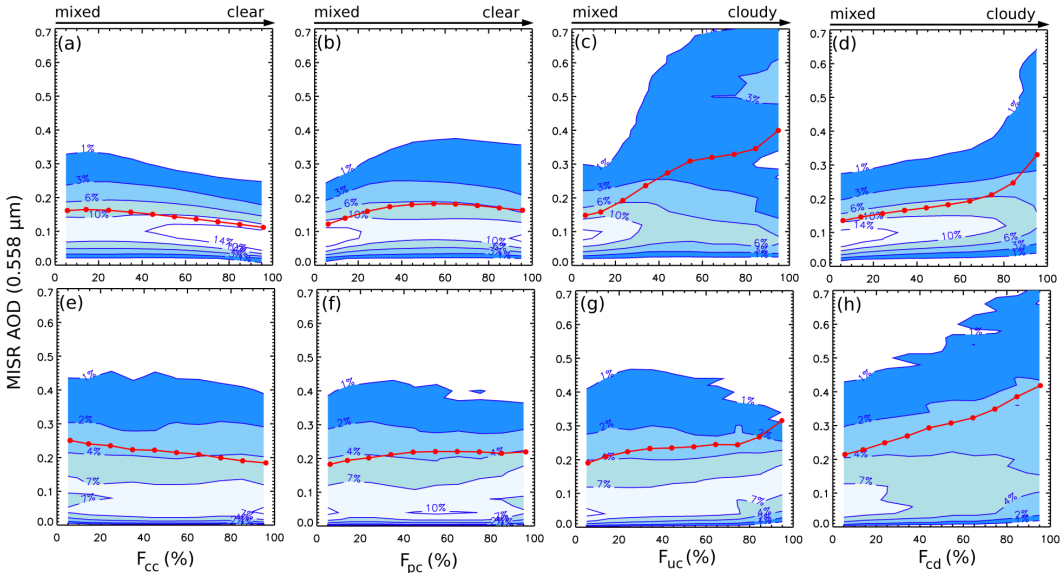

Fig. 2. MISR AOD as functions of the percentage of occurrences of the cloud flags from the MODIS cloud mask products: **(a, e)** confident clear fraction (F_{cc}), **(b, f)** probably clear fraction (F_{pc}), **(c, g)** uncertainty clear fraction (F_{uc}) and **(d, h)** cloudy fraction (F_{cd}). **(a–d)** are for the over-water data and **(e–h)** are for the over-land data. The color contour represents the fractional data density for the cloud fraction in 10 % increments. The red dots represent the mean MISR AOD within the cloud fraction bin in 10 % increments.

AMTD
6, 10057–10079, 2013

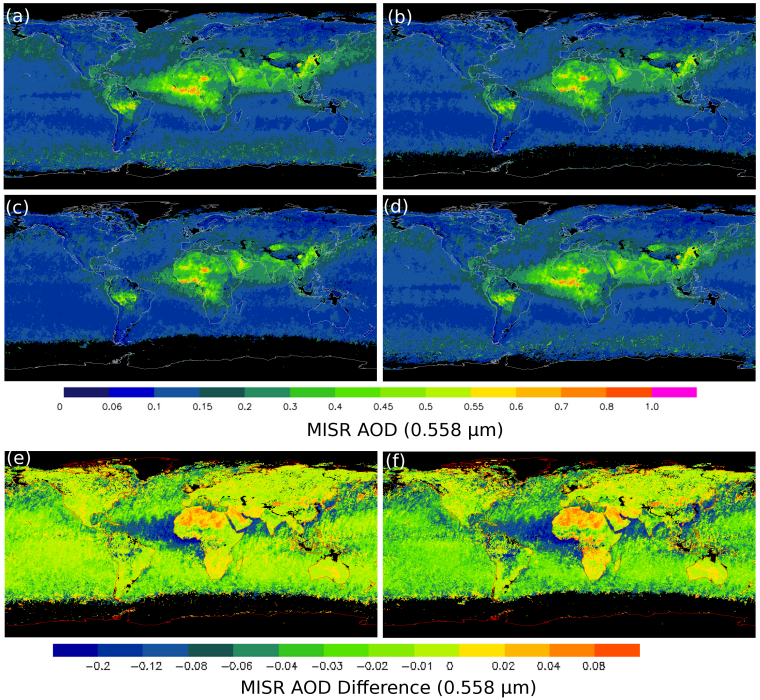

Fig. 3. Spatial distribution of MISR AOD for the 2007 dataset using the half degree (Lat/Lon) gridded level 3 MISR AOD data. **(a)** for self-QAed MISR data, **(b)** for MISR data after applying the $F_{cc} > 20\,\%$ and $F_{cirrus\_free} = 100\,\%$ cloud filters, **(c)** for MISR data after applying the $F_{cc} > 80\,\%$ and $F_{cirrus\_free} = 100\,\%$ cloud filters, **(d)** for MISR data that passed the thin cirrus cloud filter ($F_{cirrus\_free} = 100\,\%$), **(e)** AOD plot of **(b)** minus **(a)**, and **(f)** same as **(e)** but for **(c)** minus **(a)**. Color contours progressing from cold to warm represent increasing AOD values with the black color representing regions with no data.

AMTD
6, 10057–10079, 2013

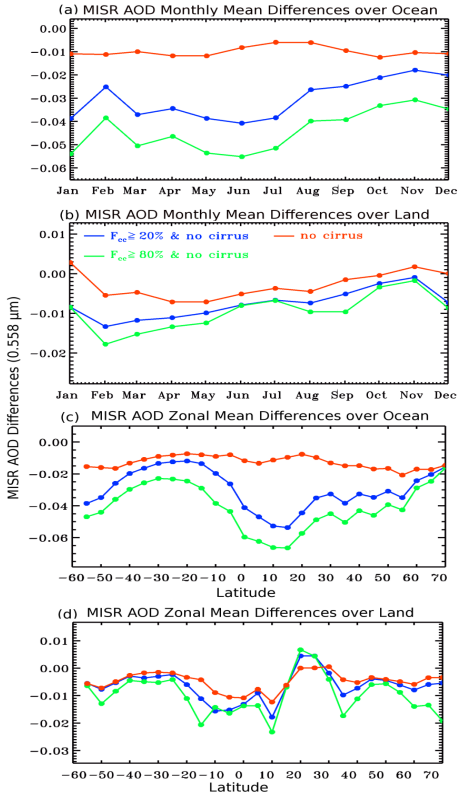

Fig. 4. MISR AOD monthly and zonal mean deviations from the self-QAed MISR AOD for 2007 (minus self-QAed). **(a)** the over-water monthly mean, **(b)** the over-land monthly mean, **(c)** the over-water zonal mean, and **(d)** the over-land zonal mean. Four data sets are plotted representing the data that passed the thin cirrus cloud filter ($F_{\text{cirrus\_free}} = 100\,\%$) in red, data that passed $F_{cc} > 20\,\%$ and $F_{\text{cirrus\_free}} = 100\,\%$ filters in blue, and data that passed $F_{cc} > 80\,\%$ and $F_{\text{cirrus\_free}} = 100\,\%$ filters in green.

AMTD
6, 10057–10079, 2013

Critical evaluation of cloud contamination in the MISR aerosol products

Y. Shi et al.